J Mater Sci (2009) 44:5494–5500
DOI 10.1007/s10853-009-3767-2

Powder metallurgical fabrication of zirconium matrix cermet nuclear fuels

Aaron R. Totemeier · Sean M. McDeavitt

Received: 19 March 2009 / Accepted: 20 July 2009 / Published online: 4 August 2009

Abstract Two powder metallurgical fabrication methods for a zirconium-based cermet nuclear dispersion fuel with oxide microspheres have been demonstrated. A multi-pass, cold-drawing process is shown to have excellent capability to control the final matrix density, though it requires several high-temperature anneals during fabrication to relieve strain hardening and increase matrix–particle bonding. Severe oxide particle damage was observed in the cold-drawn fuel pin and was likely a result of high matrix deformation resistance at room temperature. A single-pass, hot-extrusion process has been demonstrated and was shown to be capable of providing a dense matrix phase with less particle damage. Both processes were shown to be effective fabrication methods for a zirconium-based cermet, and the process variables may be controlled to create the desired fuel properties.

Introduction

Zirconium matrix cermets have been investigated as high conductivity inert matrix for two nuclear energy applications: (1) energy production with a thorium–uranium oxide ($(Th,U)O_2$) dispersion in a Zr matrix fuel [1] and (2) waste management with a uranium–transuranic (TRU) oxide ($(U,TRU)O_2$) dispersion in a Zr matrix storage form that could also be a fuel form [2]. A cermet is a two-phase composite consisting of a ceramic phase embedded in a metal matrix. Aluminum matrix cermet nuclear fuels are used extensively in research reactors around the world and stainless steel, zirconium, and tungsten matrix cermets have been explored as matrices for special application nuclear fuels for decades. Zirconium was chosen as the matrix material for both cermets described here because of its high temperature strength and corrosion resistance, well-known thermophysical properties, long history of service in the nuclear industry, and excellent neutronic properties as a non-fissionable fuel component.

In this paper, the results of two fabrication methods are presented. The first is a "cold" (room temperature) drawing process demonstrated at Argonne National Laboratory [1, 3] and the second is a high-temperature (>750 °C) extrusion process demonstrated at Texas A&M University [2]. Both processes are powder-in-tube fabrication routes and the trial experiments were performed using various oxide microspheres ($(Th,U)O_2$, ZrO_2, and $(Zr,Si)O_2$) in a zirconium metal matrix.

The cold-drawing research was completed as a fabrication demonstration for the $(Th,U)O_2$ cermet fuel form as part of a larger project funded by the U.S. Department of Energy (DOE) Nuclear Energy Research Initiative (NERI) that explored the viability of the $(Th,U)O_2$ cermet as a high burnup (i.e., deep-burn) fuel form; nuclear simulations demonstrated that a deep-burn, 10-year fuel cycle was possible. In addition, the material properties of the Zr matrix and thoria-based fuel enable direct disposal in a form that is more stable than current commercial UO_2-based fuels. The fabrication steps and preliminary behavior estimates of the cold-drawn fuel have been previously presented [1, 3], as well as nuclear and thermal modeling methods [1, 4] and a $(Th,U)O_2$ microsphere fabrication technique [1, 5]. The results described below include new information from metallurgical examination of the drawn cermet rod, which revealed significant damage to the oxide

A. R. Totemeier · S. M. McDeavitt (✉)
Department of Nuclear Engineering, Look College of Engineering, Texas A&M University, 3133 TAMU, College Station, TX 77843-3133, USA
e-mail: mcdeavitt@tamu.edu

microspheres even though the low-density zirconium matrix was well formed. The metallurgical examination was performed at Argonne National Laboratory.[1]

The hot-extrusion research focuses on the development of a transuranic (TRU) oxide storage vehicle and transmutation form. The development of the hot-extrusion method is again part of a larger NERI project [2], but this time the objective was to establish new processing methods to convert material streams from nuclear fuel recycling. The DOE has developed an aqueous separation system known as Uranium Extraction Plus (UREX+) which comprises a family of aqueous reprocessing methods with variations that may be tailored for various nuclear energy recycle applications. This project was focused on the UREX + 1a strategy wherein the final product stream is a solution of nitrates containing the transuranic isotopes of plutonium, americium, and curium. The enabling processing methods were developed to convert the UREX + 1a product streams into a U,TRU cermet [2, 6]: (1) conversion of the nuclear-grade zirconium from spent fuel cladding hulls via a hydride–dehydride method; (2) conversion of the TRU nitrate solution into oxide microspheres via internal gelation; and (3) hot extrusion of the mixed zirconium and oxide powders to form a cermet fuel pin. This extruded cermet provides a dense matrix that may serve as a safe storage form for the TRU elements but it also has potential for use as a high-burnup transmutation fuel in a fast reactor [2]. This paper describes the process variables developed for the hot-extrusion fabrication process and presents a comparison of the resulting microstructures in both cold-drawn and hot-extruded zirconium cermets.

Cermet fuels offer several advantages when compared to conventional solid–solution fuels. These benefits arise from the combined properties of both the metal and ceramic phases because each phase performs a specific task better than the other for a synergistic improvement in overall fuel performance. For example, in the proposed cermets, the matrix phase provides high strength, good thermal conductivity, and excellent corrosion resistance while porosity in the oxide microspheres can accommodate fission gases and mitigate fuel swelling while maintaining the fissionable material in a thermodynamically stable form [7]. Some of the other benefits associated with cermet dispersion fuels include increased fission gas retention, lower fuel temperatures, better containment of solid fission products, and enhanced macroscopic property retention as the fuel burnup increases. The retention of macroscopic properties with high burnup is provided by the specific geometry of the proposed cermets, consisting of spherical oxide microspheres embedded in a continuous Zr matrix.

[1] Electron microscopy by N. *Dietz Rago.*

The performance of the cermet dispersion, as with all materials, is closely related to its microstructure. A key benefit of this type of cermet dispersion is the localization of fission-induced damage in the fuel. Damage caused by nuclear decay and fission fragments creates a shell of damaged matrix material around each microsphere [8]. This allows for the design and fabrication of a fuel form that can withstand much higher burnup than solid–solution fuels as the macroscopic properties of the fuel (provided primarily by the matrix) do not deteriorate as quickly. The degree of allowable matrix damage is specific to the desired fuel [9] and the goal during fabrication should be to minimize the percentage of particles with less than a predetermined spacing. Interparticle spacing is a concern if the particles are too close and the matrix between them receives damage from multiple particles. This may not be a concern if the volume loading is low. However, if minimizing matrix damage is critical to performance, controlling the spacing may be accomplished by pre-coating the oxide particles with a layer of matrix metal.

Experimental setup

Cold drawing

The cold-drawing work is described in detail by McDeavitt et al. [1, 3] where multiple types of dispersion particles were evaluated including dense zirconia (ZrO_2) and tungsten carbide (WC) microspheres with uniform particle size distributions as well as low density spray-dried (Th,U)O_2 microspheres with approximately 20 vol.% porosity and a broad particle size distribution. The powders were dry-loaded in air into metal drawing tubes (SS316 and Zircalloy-4) and vibratory packed to 40–50% theoretical density. Each tube contained several cermet mixtures, each separated by a fine magnesium oxide powder layer within the tube. The filled tubes were drawn through a series of reducing dies to achieve the desired areal reduction. A high-temperature anneal was performed after two successive drawing passes to remove strain hardening, increase matrix density, and improve interfacial bonding of the cermet mixture.

Hot extrusion

The hot-extrusion process was developed to evaluate the effects of increased matrix plasticity during deformation. Initial experiments were designed to: (1) develop the necessary process knowledge for fabrication of lab scale specimens; (2) study the cermet behavior during processing and; (3) evaluate the finished product microstructure. In these experiments, α-phase zirconium powder (~44 μm

nominal) was used as matrix material and $(Zr,Si)O_2$ (350–500 μm) microspheres were used as surrogates for the TRU oxide microspheres (the oxide spheres were purchased as commercial yttria-stabilized ZrO_2 microspheres, but analysis revealed a significant presence of SiO_2 in the microstructure of the spheres). Due to the pyrophoric nature of the metal powder, all pre-compacted Zr powder was handled in a glovebox with a nominal argon atmosphere (i.e., the glovebox was purged with Ar and operations were carried out under a flowing Ar cover gas, but there was no atmospheric chemistry control in the system).

Powder preparation began with washing the Zr powder in ethanol to remove surface contaminants and allowing it to dry inside the glovebox. The desired amount of both powders was measured and combined in a glass vial for vibratory mixing ($\sim$10 min). The oxide powders were not pre-coated with Zr in these experiments. After mixing, the powders were loaded into a copper canister and sealed with a copper end-plug using a small lab press.

During the development of the extrusion process, several oxide volume fractions, die reductions, and temperatures were evaluated. Table 1 lists the range of the various parameters that have been tested. Various alloys were used for the extrusion tooling (NuDie® XL (H-13), Haynes® 282, Hastelloy® X, and TZM) and the design used minimal components, including a die, a billet holder, and an extrusion ram. The dies were conical reduction dies using a reduction half-angle of 45°. A 100-ton hydraulic press was used to supply the extrusion pressure. Ceramic fiber heaters (Watlow®) were used to heat the green billet and the extrusion tooling to $\sim$800 and 550 °C, respectively. Two heaters were arranged such that the billet was heated immediately above the tooling heater, separated by an insulating board. When the desired soak temperature was achieved, the billet could be transferred into the billet holder through a pass-through in the insulating board and the extrusion began. Figure 1 shows a photograph the extrusion press with the heaters as well as a schematic diagram of the extrusion system.

Table 1 Hot-extrusion development test parameters

Parameters	Parameters tested
Cermet components	
Zr (μm nominal)	44
$(Zr,Si)O_2$ (μm nominal)	500
Die reduction	2.67 (62.4%)
$R = A_o/A_f$ (areal reduction)	6 (83.3%)
	9 (88.9)
Die angle (half angle)	90° (45°)
Oxide volume fraction	0.1–0.4
Tool material	
Die	H-13 and TZM
Billet holder	H-13 and Hastelloy X
Extrusion ram	H-13 and Haynes-282®
Billet temperature	600–850 °C
Tool Temperature	400–650 °C

Metallurgical observations

Structure of Zr–UO_2–ThO_2 cermet

The cold-drawn fuel pin presented in this paper consisted of spray-dried oxide microspheres (25 wt% ThO_2, 25 wt% UO_2) with 50 wt% Zr in SS304 cladding. The fuel pin length was $\sim$44 cm from which two pieces were sectioned for analysis. The specimen appeared to consist of two interspersed phases, a shiny metallic phase and a yellowish white phase consisting of compacted particles. The matrix material was dense and well-formed; however, the oxide particles were pulverized, most likely during deformation, and easily pulled out of the matrix during polishing. This is evidenced by deep cavities that were pulled out from the cermet during polishing and are clearly visible. To mitigate oxide pullout, no polishing beyond 1200 grit SiC paper was performed on this specimen.

Figure 2 is a secondary electron image of the microstructure, which provides some detail into the extent of damage incurred within the oxide particles. The pre-drawn oxide had been sieved to have a uni-modal size distribution with a nominal particle size of 200 μm. However, fine $(Th,U)O_2$ particles are present at the matrix grain boundaries throughout the drawn material as observed via scanning electron microscopy (SEM) in Fig. 3, the compositions were confirmed using energy dispersive spectroscopy (EDS). It is likely that this fine dispersion was initiated during the initial reduction after the oxide particles were pulverized with continued damage as the drawing process proceeded. Sub-micron oxide particles are observed throughout the Zr matrix; many of the oxide-inhabited grain boundaries extend far away from regions of high oxide concentration. Grain boundary diffusion of the oxide is not likely during room temperature fabrication.

The extensive oxide damage observed in this specimen is not uncommon to the other cold-drawn specimens produced in this earlier study, but these observations from the actual $(Th,U)O_2$ were not previously available. The oxide damage is clearly due to the combination of high stress and low temperature associated with the cold-drawing process. On the other hand, the damage seen in the $(Th,U)O_2$ "spheres" is far more extensive than that observed in the previously reported ZrO_2 and WC spheres. These spheres were fabricated by spray drying and sintering [5] and it is likely that the high porosity and particle irregularities contributed to the weakness of the microspheres.

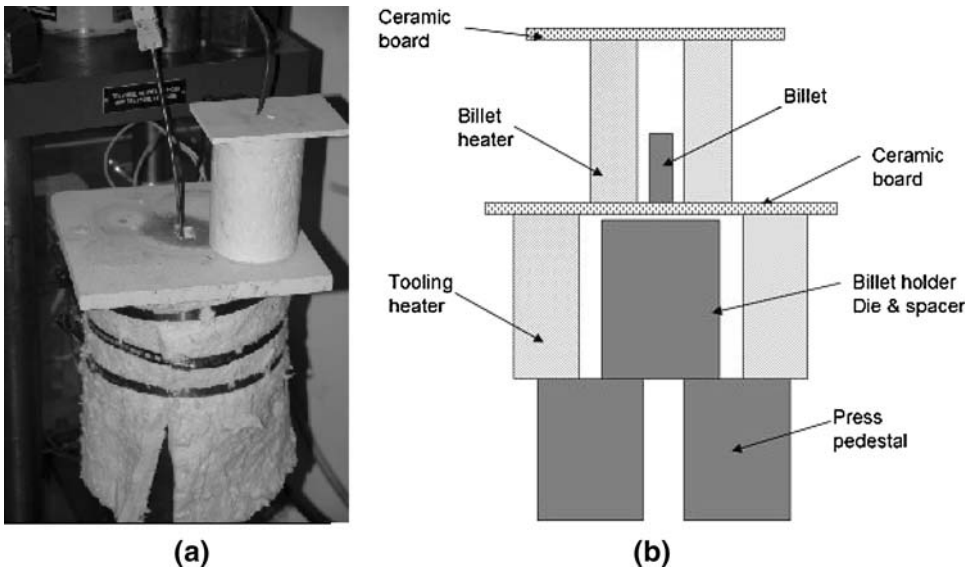

Fig. 1 Hot-extrusion equipment **a** system photograph and **b** schematic diagram of the process

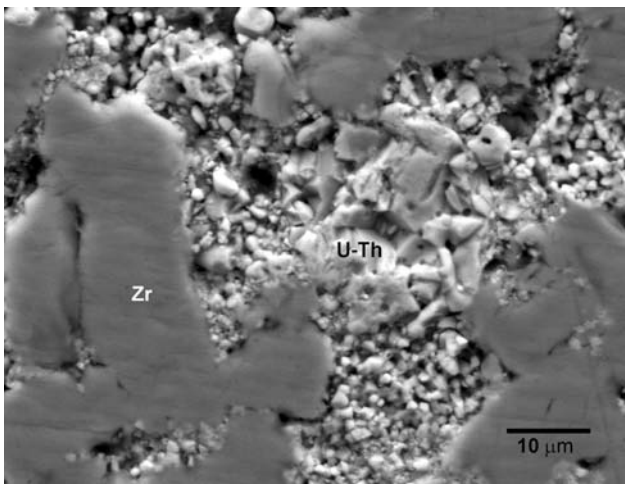

Fig. 2 Secondary electron image of the cold-drawn $(Th,U)O_2$–Zr cermet detailing the damage to oxide particles from drawing; many oxide fragments exhibit porosity

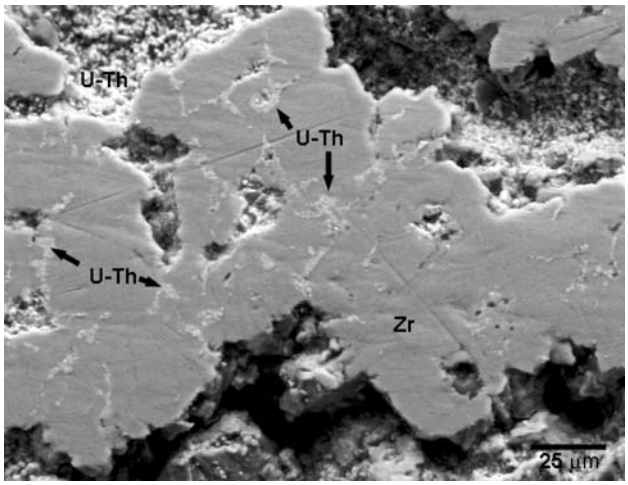

Fig. 3 Secondary electron image of the cold-drawn $(Th,U)O_2$–Zr cermet showing fine oxide dispersions present in the grain boundaries of the zirconium matrix

Structure of hot-extrusion matrix

Not all of the extrusion development tests covered in Table 1 produced successful extrusions. The initial tests described here were performed as a scoping study to determine the necessary parameters to be used for future work. As such, two extrusions (areal reductions of 88 and 62%) are discussed here which show the general features of the extruded matrix. The 88% reduction cases resulted in a dense metal matrix suggesting good matrix compaction during reduction. However, the stresses developed during these high reduction extrusions resulted in extensive particle damage for oxide loadings higher than 30 vol.%. Figure 4 shows an extruded specimen with 30 vol.% oxide (initial billet temperature of 845 °C). In the central region of the cermet, particles appear damaged due to stress buildup between two or more particles, resulting in a crack through the particles generally beginning along the axis of closest approach. The oxide particle damage in Fig. 4 is more severe near the radial exterior of the extruded rod (top and bottom of figure) as this region undergoes the highest deformation shear and axial displacement during extrusion, see Fig. 5. A high concentration of pulverized particles, elongated along the extrusion direction, is present in these regions. Matrix flow around the particles is better in the central region of the cermet than in the outer regions. The large amount of deformation along the extrusion direction experienced by the outer regions may be too severe to allow for full particle encapsulation. The central region also exhibits poor matrix bonding, to a lesser extent, and

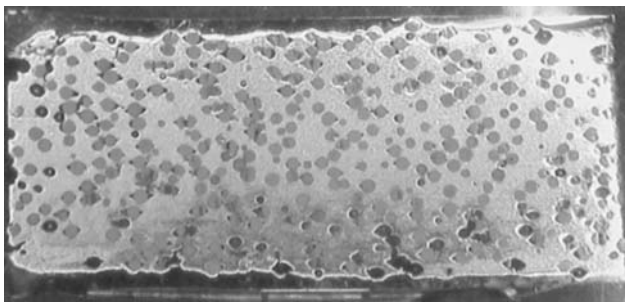

Fig. 4 Optical micrograph of extruded cermet (88% areal reduction and 845 °C extrusion). Total length of extruded section is 0.5 in. Higher magnification is shown in Fig. 5

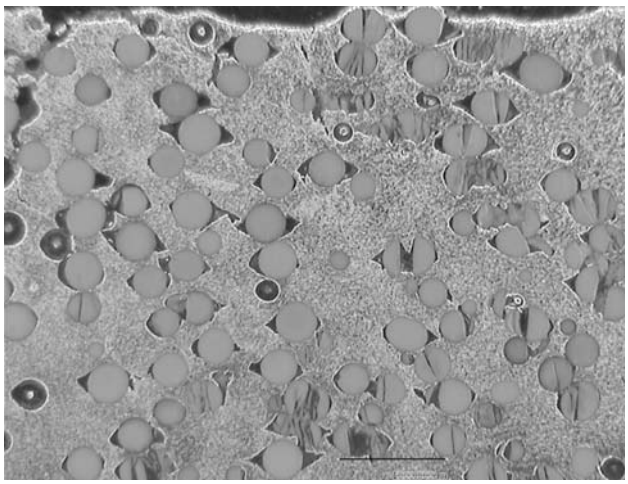

Fig. 5 Optical micrograph of extruded cermet from Fig. 4 showing severe particle damage in outer regions (top and bottom) of cermet rod (88% areal reduction and 845 °C extrusion). Scale bar is 1 mm

appears to be prevalent in regions where particles are in close proximity to one another.

The 62% areal reduction was performed with 16 vol.% oxide loading and an initial billet temperature of 850 °C to reduce particle damage. The resulting cermet is shown in Fig. 6. During preparation for microscopic analysis, a large amount of Zr powder was found in the polishing fluid and many oxide particles were pulled out of the cermet suggesting poor matrix densification at this low areal reduction. Further evidence of poor matrix flow is evidenced by the large cracks in the cermet matrix and in the gaps formed around the oxide particles (Fig. 7). This suggests that the areal reduction was too small for dense matrix formation. There is little evidence of particle pulverization due to high shear zones though fractured particles are present in this specimen. The overall damage concentration is substantially lower than in the specimen with higher loading and reduction. As observed in Fig. 7, matrix flow around particles that are closely spaced is very poor.

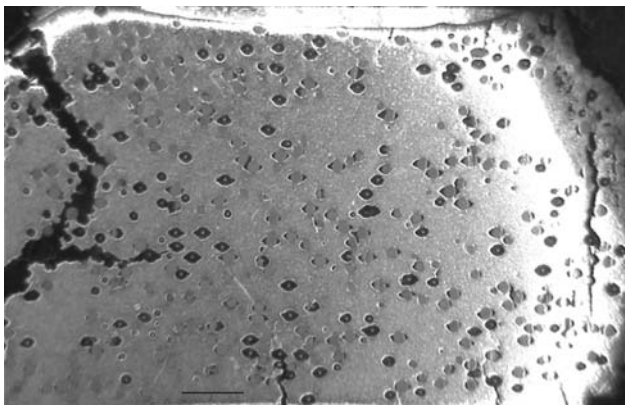

Fig. 6 Optical micrograph of extruded cermet showing poor matrix densification, cracks, and oxide pullout (62% areal reduction and 850 °C extrusion). Extruded specimen is ~0.75 in long. Higher magnification is shown in Fig. 7

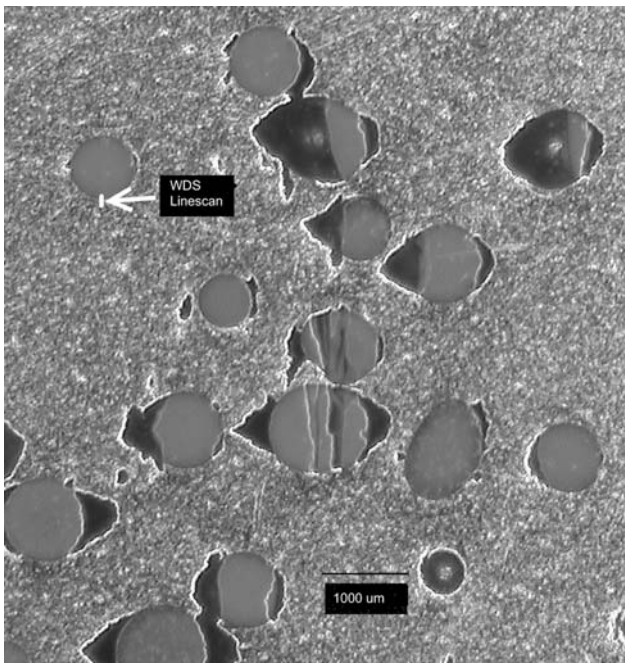

Fig. 7 Optical micrograph of extruded cermet is shown in Fig. 6 (62% areal reduction and 850 °C). Matrix bonding is poor as large gaps are present around the oxide microspheres and matrix porosity is high. A representative region of the WDS linescan is also shown in the figure

Particle–matrix interface after hot extrusion

One concern with the hot-extrusion process is the potential for zirconium to reduce the oxide microspheres. This could lead to the formation of a weak interaction layer around the microspheres which would inhibit the thermal conductivity between the matrix and particle and possibly (depending on the fuel phase formed after reduction) to localized fuel melting. To evaluate this concern, the oxide–matrix

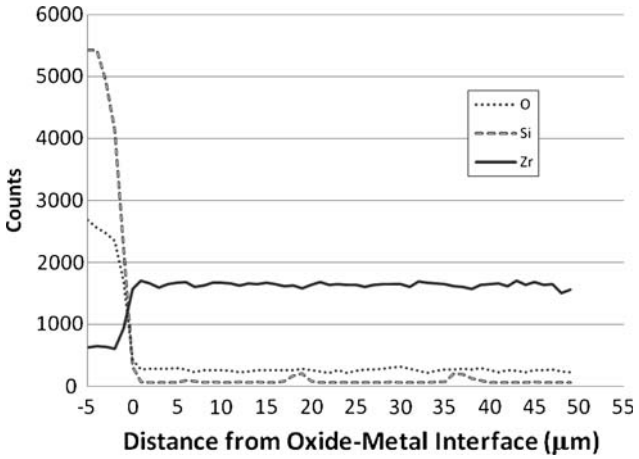

Fig. 8 Depth profile element map from wavelength dispersive spectroscopy across the interface between an $(Zr,Si)O_2$ particle and the Zr matrix after extrusion at 850 °C

interface of the 88% areal reduction specimen was analyzed with wavelength dispersive spectroscopy (WDS); a representative location for the WDS linescan is shown in Fig. 7 crossing from the oxide phase to the metal phase. The pre-extruded billet for this specimen was heated from room temperature to 850 °C in approximately 1 h and held at the extrusion temperature for ~20 min. The chart in Fig. 8 shows the relative amounts of Zr, Si, and O across the interface of the particle into the matrix. It can be seen that oxygen concentration drops off within a few microns of the interface. This indicates that particle–matrix chemical interactions will be negligible during hot extrusion but further study is required to understand the importance of this phenomenon at fuel operating temperatures under radiation conditions.

Summary of observations

Both the cold-drawing and hot-extrusion routes are viable fabrication processes for zirconium matrix cermets, but both methods have significant issues with oxide particle destruction that need to be managed in the context of the particular dispersion material selected for a given application. Continued development of either process is required before they can be implemented as a fuel fabrication technique.

The cold-drawing process provides excellent control over the final matrix density by allowing the user to design the final rod diameter by changing the number and degree of reduction passes. This fine control over the final fuel density exists because the densification from drawing comes primarily from radial compression; specification of the areal reduction profile specifies the final cermet density. The low temperatures of cold drawing do not enable low-stress flow of the matrix and thus weak oxide particles such as the low density $(Th,U)O_2$ observed here will be easily pulverized during fabrication. In the example described above, the $(Th,U)O_2$ powders were severely damaged during processing and the original morphology was lost. There may be nuclear fuel applications where this type of fine dispersion is desirable, but that was not the target of the work described above.

The two extrusion pins represented in this paper depict the extremes of matrix density. The 88% reduction yielded a very dense matrix with severe particle damage while the 62% reduction produced a weak matrix without full encapsulation of the oxide phase. Neither extreme would be an acceptable nuclear fuel form but an acceptable form is feasible between these extremes. Even so, it does appear that extrusion would be best suited for low oxide volume fractions (i.e., below 30 vol.%). Smaller oxide particles could allow for improved matrix contact around particles that are closely spaced and a reduction in the stresses developed in the regions of high deformation. Hot extrusion is generally complicated because the temperatures involved produce the need for high strength die materials. That being said, the TZM and superalloy materials selected for this study worked well. The forces involved in extrusion are both radial and axial, as the material is being pushed through the die from behind, so the material flow profile through the die is different than drawing and the resulting matrix can be very dense.

One of the primary benefits of cermet dispersion fuels is the localization of radiation damage effects due to fission. Destruction of the oxide microspheres to the extent observed in the cold-drawn fuel pin and high reduction extruded pin is not desirable for favorable fuel performance, as the cermet would lose the benefit of localized fission-induced damage. Some particle destruction is expected and manageable (e.g., particle cracking) but a quantifiable degree of acceptable destruction requires further analysis.

Further investigation on the impact of oxide particle density on final integrity should be performed. Fuel swelling from accumulated fission gases at high burnup may be mitigated using oxide particles of 70–80% TD (theoretical density). The density of the $(Th,U)O_2$ particles used for cold drawing was nominally around 80% TD. It is likely that the density of these particles was a contributor to the severity of damage observed. The $(Si,Zr)O_2$ particles used in the extrusion work had a measured density of ~95% TD but such a density in a $(U,TRU)O_2$ particle would not be effective at accommodating fission gas buildup. If either process was chosen as a fabrication method, the specific process parameters for the desired fuel would need to be determined.

Future work on Zr matrix fuels for TRU burning should focus on (1) optimizing the processing temperature to achieve good Zr flow with minimal physical or chemical damage to the oxide fuel, (2) the optimization of the zirconium powder and oxide particle size to achieve gentler extrusion stresses, and (3) the inclusion of lower density oxide spheres to simulate real fuel particles.

Acknowledgements The authors would like to thank Nancy Dietz-Rago of Argonne National Laboratory (ANL) for providing the microscopic images from the cold-drawn specimen and Dr. R. Guillemette of Texas A&M University for the WDS analysis on the extruded specimen. Previous collaborators in $(Th,U)O_2$ cermet fabrication include M.C. Hash and A.S. Hebden at ANL and Prof. A.A. Solomon at Purdue University who are gratefully acknowledged. Also, the authors wish to acknowledge the U.S. Department of Energy for funding the work described here under the Nuclear Energy Research Initiative (Project No. 05-066 for the hot-extrusion work and Project No. 99-095 for the cold-drawing work).

References

1. McDeavitt SM, Xu Y, Downar TJ, Solomon AA (2007) Nucl Technol 157(1):37
2. McDeavitt SM, Parkison AJ, Totemeier AR, Wegener JJ (2007) Mater Sci Forum 561–565:1733
3. McDeavitt SM, Downar TJ, Revankar S, Solomon AA, Hash MC, Hebden AS (2002) Thoria-based cermet nuclear fuel: cermet fabrication and behavior estimates. American Society of Mechanical Engineers, Arlington, VA, ICONE10-22317
4. Downar TJ, McDeavitt SM, Kim TK, Solomon AA (2002) Thoria-based cermet nuclear fuel: neutronics fuel design and fuel cycle analysis. American Society of Mechanical Engineers, Arlington, VA, ICONE10-22305
5. Solomon AA, McDeavitt SM, Chandramouli V, Anthonysamy S, Kuchibhotla S, Downar TJ (2002) Thoria-based cermet nuclear fuel: sintered microsphere fabrication by spray drying. American Society of Mechanical Engineers, Arlington, VA, ICONE10-22445
6. McDeavitt SM, Kramer DT, Parkison AJ, Totemeier AR, Wegener JJ (2005) Zirconium matrix cermet storage form and transmutation fuel for transuranics, vol 93. American Nuclear Society Transactions, La Grange Park, IL, p 743
7. Lambert JDB (1968) Irradiation Study of UO_2-stainless steel and $(Pu, U)O_2$-stainless steel cermet fuels in rod and plate geometries. High Temp Nucl Fuels 42:237–254
8. Fernandez A, Konings RJM, Somers J (2003) Design and fabrication of specific ceramic-metallic fuels and targets. Elsevier, Tokai, Japan
9. Holden AN (1967) Dispersion fuel elements. Gordon and Breach Science Publishers, New York